# Unperverted synthesis of complex sphingolipids is essential for cell survival under nitrogen starvation

**Maki Yamagata[1], Keisuke Obara[1], and Akio Kihara[1,*]**

[1]*Faculty of Pharmaceutical Sciences, Hokkaido University, Sapporo 060-0812, Japan*

Short title: Role of sphingolipids under starvation

[*]Correspondence:

Akio Kihara, PhD

Faculty of Pharmaceutical Sciences, Hokkaido University

Kita 12-jo, Nishi 6-chome, Kita-ku, Sapporo 060-0812, Japan

Tel: +81-11-706-3754

Fax: +81-11-706-4900

E-mail: kihara@pharm.hokudai.ac.jp

Keywords: sphingolipid; lipid; nitrogen starvation; vacuole; calcium ion

**Abstract**

Changes in membrane dynamics are known to occur in cells faced with starvation. However, the functions of the major lipid components of biological membranes, sphingolipids, during the starvation response remain unclear. In this study, we found that yeast cells lacking genes encoding mannosylinositol phosphorylceramide (MIPC) synthases (*csg1*Δ *csh1*Δ) underwent rapid cell death upon nitrogen starvation, but not upon carbon starvation or carbon and nitrogen starvation. Addition of $NaN_3$ prevented the nitrogen starvation-induced cell death of the *csg1*Δ *csh1*Δ cells, indicating that energy production is required for this rapid cell death. The cell death was caused by an accumulation of inositol phosphorylceramide (IPC) species containing phytosphingosine. Removing $Ca^{2+}$ by treating the cells with a calcium chelator or by changing the medium to a $Ca^{2+}$-free medium prior to nitrogen starvation rescued the cells from death. Approximately half of the cells died shortly after collapse of the vacuole, while in the other half morphological changes in the cytoplasm preceded vacuole disruption. Since the vacuole is the major $Ca^{2+}$-storage organelle, we hypothesize that the vacuole is involved in the cell death either directly or indirectly. We report here that normal synthesis of complex sphingolipids is important for cell survival in nitrogen-starved medium.

**Introduction**

Under nutrient-starved conditions, cells draw on a variety of responses to survive, including large changes in membrane dynamics. For example, in yeast secreted proteins are redirected to the vacuole for degradation (van der Rest *et al.* 1995). In some cells autophagy is induced, in which newly-synthesized double membrane structures, called autophagosomes, engulf cytoplasmic constituents and deliver them to the vacuole (in yeast) or lysosome (in mammals) (Ohsumi 1999). In the vacuole/lysosome, biological macromolecules are degraded to low-molecular weight compounds for recycling. To date, more than 30 proteins required for autophagy have been identified and extensively analyzed (Tsukada & Ohsumi 1993; Thumm *et al.* 1994; Klionsky *et al.* 2003).

In contrast to the findings above, knowledge regarding roles in starvation for lipids is still limited. Sphingolipids are major lipid components conserved in eukaryotes, from yeast to mammals. These lipids play many important functions in cells, including functions in membrane trafficking, cell adhesion, skin barrier formation, immunity, and glucose tolerance (Kihara *et al.* 2007; Mizutani *et al.* 2009; van Meer & Hoetzl 2010; Hla & Dannenberg 2012). The hydrophobic backbone of sphingolipids, ceramide, is composed of a long-chain base and an amide-linked fatty acid. In mammals, the polar head groups are phosphocholine for sphingomyelin, or for glycosphingolipids, any of hundreds of sugar chains differing in the number and/or linkage positions of sugars. In the budding yeast *Saccharomyces cerevisiae*, however, the head group composition for sphingolipids is comparatively simple, so this yeast has been widely used as a model organism for sphingolipid research.

Only three types of complex sphingolipids exist in *S. cerevisiae*, inositol phosphorylceramide (IPC), mannosylinositol phosphorylceramide (MIPC), and mannosyldiinositol phosphorylceramide ($M(IP)_2C$) (Fig. 1) (Dickson *et al.* 2006). IPC is a precursor for MIPC and the further metabolite $M(IP)_2C$. Disruption of the gene encoding IPC synthase, *AUR1*, causes loss of all complex sphingolipids, and *AUR1* is known to be essential for cell growth (Nagiec *et al.* 1997). MIPC, in contrast, is synthesized by two MIPC synthases, Csg1 and Csh1 (Beeler *et al.* 1997; Uemura *et al.* 2003). Deletion of the *CSG1* gene causes greatly reduced MIPC synthesis, whereas deleting *CSH1* has no effect (Uemura *et al.* 2003). Deletion of both genes results

in the complete abolishment of MIPC, yet the double mutant cells grow normally. Likewise, disruption of the *IPT1* gene, which encodes $M(IP)_2C$ synthase, does not impair growth (Dickson *et al.* 1997). Thus, MIPC and $M(IP)_2C$ are dispensable for growth under normal conditions, but they seem to be required for growth under stressful conditions, or they may be involved in adaptation to environmental changes. In fact, deletion of either *CSG1* or *IPT1* causes altered sensitivities to $Ca^{2+}$ ions, oxidative stress, acidic pH, drugs, or toxins (Beeler *et al.* 1997; Im *et al.* 2003; Zink *et al.* 2005; Aerts *et al.* 2006; Mira *et al.* 2009; Alamgir *et al.* 2010).

The *CSG1* and *CSG2* genes were identified as genes that exhibit high sensitivities to exogenous $Ca^{2+}$ when mutated (Beeler *et al.* 1994; Beeler *et al.* 1997). Csg2 was later demonstrated to be a regulatory subunit of each of the two redundant MIPC synthases, Csg1 and Csh1 (Uemura *et al.* 2003). Disruption of the *CSG2* gene causes large decreases in Csg1 activity and abolishes Csh1 activity altogether (Uemura *et al.* 2003). Several lines of evidence have indicated that an accumulation of IPC in the *CSG2* deletion mutants causes $Ca^{2+}$ sensitivity, and that this is especially true for accumulation of IPC having a hydroxyl group at the C-4 position on the long-chain base moiety (*i.e.*, phytosphingosine) (Zhao *et al.* 1994; Haak *et al.* 1997). Conversely, deletion of the *SUR2* gene, which encodes the C4-hydroxylase responsible for phytosphingosine production, reduces the $Ca^{2+}$ sensitivity of the *CSG2* deletion mutant (Dunn *et al.* 1998). The reason why exogenous $Ca^{2+}$ causes toxicity through IPC still remains unclear.

We previously reported that in yeast sphingolipid synthesis is required for autophagy induced by simultaneous depletion of nitrogen and carbon sources (Yamagata *et al.* 2011). Treatment with myriocin, an inhibitor of the serine palmitoyltransferase that catalyzes the first step of sphingolipid synthesis, or with the Aur1 inhibitor aureobasidin A results in reduced autophagic activities. In contrast, neither double deletions in *CSG1* and *CSH1* nor a deletion in *IPT1* affects autophagy. These results suggest that IPC, but not MIPC or $M(IP)_2C$, is required for autophagy induced by depletion of nitrogen and carbon sources (Yamagata *et al.* 2011). In the course of that study, we observed that double mutant cells lacking both *CSG1* and *CSH1* underwent rapid cell death under nitrogen-deprived (but carbon-containing) conditions. In the study presented here, we investigated the molecular mechanisms of that rapid cell death and found that IPC

containing phytosphingosine and intracellular $Ca^{2+}$ ions are involved.

## Results

### A MIPC synthase mutant rapidly dies under nitrogen-starved conditions

To examine the roles of sphingolipids in starvation, cells deficient in MIPC synthase (*csg1*Δ *csh1*Δ) were grown in various nutrient-deprived media. Nearly all wild type cells were still alive 24 hr after the shift to any of the nutrient-deprived media tested, i.e., nitrogen- (SD(-N)), carbon- (S(-C)), or nitrogen- and carbon-starved medium (S(-NC)). However, *csg1*Δ *csh1*Δ cells rapidly died in SD(-N) medium (Fig. 2A and B), with ~90% cell death after 4 hr. Dead cells were visualized by staining with the pigment phloxine B, which indicates a loss of efflux activities. In addition, dead cells were morphologically smaller, which allowed us to readily distinguish them from living cells by observation under a phase-contrast microscope. Twenty-four hr after a shift to SD(-N) medium, nearly all *csg1*Δ *csh1*Δ cells had died (Fig. 2B). This cell death was not caused by osmotic shock, since addition of 1 M sorbitol in the medium had no effect (data not shown).

Under starvation conditions, autophagy is induced to degrade the cell's own constituents for recycling. Therefore, nutrient shortage is more severe in autophagy-deficient cells than in wild type cells. However, autophagy-deficient cells (*atg14*Δ) survived for 24 hr in SD(-N) medium (Fig. 2B), which was consistent with a previous study that autophagy-deficient cells usually begin to die after 2-3 days of starvation (Tsukada & Ohsumi 1993). These results suggest that the rapid cell death of *csg1*Δ *csh1*Δ cells is not caused by the nutrient shortage but rather through a failure of early cellular responses to nitrogen starvation.

Although *csg1*Δ *csh1*Δ cells were highly sensitive to nitrogen starvation, they were resistant to carbon starvation (in S(-C) medium) and to carbon and nitrogen starvation (in S(-NC) medium). To examine in more detail the effect on cell survival of glucose present in the nitrogen starvation medium, *csg1*Δ *csh1*Δ cells were subjected to nitrogen starvation in the presence of various glucose concentrations. Increasing the glucose concentration in the SD(-N) medium resulted in decreases in the number of living cells in a dose-dependent manner (Fig. 2C). These results suggest that sphingolipids are involved in cell survival only under nitrogen-depleted conditions, and that glucose is a negative effector for this cell death.

In the presence of glucose, cells can produce energy even under nitrogen-starved conditions. To examine whether the effect of glucose was linked to energy production, we examined the cell death of *csg1*Δ *csh1*Δ cells in the presence of $NaN_3$, which inhibits energy production, under nitrogen-starved conditions. Addition of $NaN_3$ to the medium suppressed the rapid cell death almost completely (Fig. 2D). Thus, energy production is required for the rapid cell death of *csg1*Δ *csh1*Δ cells in nitrogen-starved medium.

After approximately 4 hr of nitrogen starvation, autophagy is actively ongoing. To examine whether autophagy is involved in the cell death of the MIPC synthase mutant, we created *csg1*Δ *csh1*Δ *atg14*Δ cells and subjected them to nitrogen starvation. Rapid cell death was still observed for the triple mutant, similar to results observed for *csg1*Δ *csh1*Δ cells (Fig. 2E). Thus, autophagy is not responsible for the rapid cell death of *csg1*Δ *csh1*Δ cells under nitrogen starvation.

**IPC containing phytosphingosine is involved in the death of *csg1*Δ *csh1*Δ cells under nitrogen-deprived conditions**

In *csg1*Δ *csh1*Δ cells, MIPC is absent, but its precursor, IPC, is accumulated. To discriminate whether absence of MIPC or accumulation of IPC is involved in the rapid cell death, we examined the effect of myriocin, an inhibitor for *de novo* sphingolipid synthesis, on the cell death of *csg1*Δ *csh1*Δ cells in SD(-N) medium. Myriocin greatly reduced the cell death of the *csg1*Δ *csh1*Δ cells at 4 hr (Fig. 3A). Twenty-four hr incubation in starvation medium in the presence of myriocin caused cell death of wild type cells (to ~20% alive), probably due to the absence of sphingolipids. The cell survival rate of the *csg1*Δ *csh1*Δ cells at 24 hr was comparable to that of wild type cells. Since myriocin treatment leads to a decrease in all sphingolipid species, including IPC, these results indicate that the accumulation of IPC, and not the absence of MIPC, has a role in the rapid cell death under nitrogen starvation conditions.

*S. cerevisiae* contain five IPC species differing in the number and/or positions of hydroxyl groups on the ceramide moiety (Beeler *et al.* 1997; Haak *et al.* 1997). The hydroxylases Sur2 and Scs7 and the copper transporter Ccc2 are known to be involved, either directly or indirectly, in these hydroxylations (Beeler *et*

*al.* 1997; Haak *et al.* 1997). To examine which type of IPC is the most effective for the rapid cell death, a *sur2*Δ, *scs7*Δ, or *ccc2*Δ mutation was introduced into *csg1*Δ *csh1*Δ cells. When the *csg1*Δ *csh1*Δ *sur2*Δ cells were grown in SD(-N) medium, their survival rate was greatly improved compared to the original *csg1*Δ *csh1*Δ cells (Fig. 3B). On the other hand, the *scs7*Δ or *ccc2*Δ mutation had little or no effect on the cell death of the *csg1*Δ *csh1*Δ cells. Sur2 catalyzes the conversion of the long-chain base dihydrosphingosine to phytosphingosine, by adding one hydroxyl group at the 4 position of dihydrosphingosine. Therefore, phytosphingosine-containing IPC is the causative lipid molecule that leads to cell death under nitrogen-starved conditions.

**Intracellular $Ca^{2+}$ ions are responsible for the death of *csg1*Δ *csh1*Δ cells under nitrogen-starved conditions**

Studies have reported that MIPC-decreased or -deficient cells, including *csg1*Δ, *csg2*Δ, and *csg1*Δ *csh1*Δ cells, are sensitive to high $Ca^{2+}$ ion concentrations (Beeler *et al.* 1994; Beeler *et al.* 1997; Uemura *et al.* 2003). The $Ca^{2+}$-sensitive phenotype of *csg2*Δ cells could be suppressed by certain mutations that cause a reduction in the levels of IPC containing phytosphingosine, such as the *sur2*Δ mutation (Haak *et al.* 1997). Due to the resemblance, we speculate that the cell death of *csg1*Δ *csh1*Δ cells described in those reports is somewhat related to the cell death described here (Fig. 2A and B), although there are differences in the media used (nutrient-rich medium versus nitrogen-deprived medium) and in the exogenous $Ca^{2+}$ concentration (50 mM versus no extra addition (in SD medium, ~1 mM $Ca^{2+}$)). To examine the possibility that $Ca^{2+}$ ions are also involved in the rapid cell death of *csg1*Δ *csh1*Δ cells under nitrogen starvation, *csg1*Δ *csh1*Δ cells were grown in SD(-N) medium containing the $Ca^{2+}$-chelator EGTA. Although neither 1 mM nor 3 mM EGTA had much effect on cell survival, 10 mM EGTA greatly suppressed cell death (Fig. 4A). Considering that the $Ca^{2+}$ concentration present in the medium was only ~1 mM, and a high EGTA concentration was required to elicit the effect on the cells, it is highly likely that chelating the intracellular $Ca^{2+}$ (by endocytosed EGTA) and not the $Ca^{2+}$ ions in the medium, was responsible for the suppression of cell death.

We next investigated cell survival in $Ca^{2+}$-free medium. When *csg1*Δ *csh1*Δ cells were cultured in SC medium (containing $Ca^{2+}$) and then shifted to nitrogen-deprived medium lacking $Ca^{2+}$ (SD(-N)-$Ca^{2+}$), most of the cells still underwent rapid cell death (Fig. 4B). However, when cells were cultured in SC medium lacking $Ca^{2+}$ (SC-$Ca^{2+}$) and then shifted to SD(-N)-$Ca^{2+}$ medium, the cell survival rate was greatly increased (Fig. 4B). These results indicate that intracellular $Ca^{2+}$ accumulated prior to nitrogen starvation is involved in the death of *csg1*Δ *csh1*Δ cells.

**The yeast vacuole plays a role in the death of *csg1*Δ *csh1*Δ cells under starvation conditions**

In yeast, the vacuole is the major $Ca^{2+}$ storage organelle. Therefore, we speculate that the vacuole is involved in nitrogen starvation-induced cell death. To monitor the vacuole under nitrogen-deprived conditions, wild type and *csg1*Δ *csh1*Δ cells were stained with FM4-64, a lipophilic fluorescent dye that stains the vacuolar membrane. After a 2.5 hr culture, most of the wild type cells in either rich medium or nitrogen-deprived medium, and most of the *csg1*Δ *csh1*Δ cells in rich medium were living, and their vacuoles were observed as FM4-64-stained, red membrane structures (Fig. 5A). On the other hand, approximately 65% of the *csg1*Δ *csh1*Δ cells incubated in SD(-N) had died by 2.5 hr, and the FM4-64 signal was lost in these dead cells, indicating that the vacuole had been disrupted.

To determine whether the vacuole disruption occurred before or after the cell death, we monitored vacuole integrity by staining the vacuole lumen with dichlorofluorescein diacetate (DCFDA), which yields fluorescence under acidic conditions. MIPC synthase-deficient cells were stained with DCFDA under nitrogen starvation and observed by fluorescence microscopy. Photographing individual cells every 2 min enabled us to observe morphological changes in the vacuole and the cell around the time of cell death. We obtained photographs of 22 examples of dying cells and could classify the cell death pattern into 2 (pattern I and pattern II), each having 11 examples. In pattern I, cells appeared to die shortly after vacuole disruption. One photograph captured the exact moment of vacuole disruption (0 min, Fig. 5B, upper panels) and DCFDA flowing out of the vacuole; by 2 min the DCFDA signal was observed throughout the cell. Since DCFDA becomes fluorescent under acidic conditions, fluorescence throughout the cell indicates

that the acidic contents normally stored in the vacuole had been released into the cytoplasm. The high DCFDA signal was prolonged up to 8 min. From 10 to 16 min, the DCFDA signal gradually declined, suggesting that the DCFDA and/or cellular contents leaked out of the cell due to plasma membrane disruption. In phase contrast imaging, the cell morphology appeared unchanged up to 10 min. However, by 12 min cells had undergone final morphological changes, in which the cytoplasm became small and the cellular organelles could not be distinguished.

In pattern II, the cytoplasm of the nitrogen-deprived cells first became transparent and small, reminiscent of plasma membrane collapse (Ohsumi *et al.* 1988), then the vacuole was disrupted. One example of cells undergoing pattern II cell death exhibited transparent cytoplasm at 0 min, at which time the vacuole was slightly swollen (Fig. 5B, lower panels). By 6 min the cell had undergone the final morphological change, so the vacuole was disrupted, the DCFDA signal was spread over the cytoplasm, the cell was small, and the cellular organelles could not be distinguished. The time lag between cytoplasm becoming transparent and the final morphological change varied among the examples in pattern II (0 min to > 30 min). This was in contrast to the vacuolar disruption and final morphological changes observed in pattern I, which occurred almost uniformly within 10 min. Although the precise mechanism of pattern II death is unclear, at least half of the cells (pattern I) appeared to die due to vacuole disruption.

## Discussion

In the presented study, we found that cells lacking MIPC synthases (*csg1*Δ *csh1*Δ) rapidly die in SD(-N) medium (Fig. 2A and B). This cell death is not caused by a nutrient shortage (Fig. 2B), but rather by an accumulation of phytosphingosine-containing IPC (Fig. 3A and B). Thus, normal conversion of IPC to more complex sphingolipids is necessary to survive under nitrogen-starved conditions. We also revealed here that intracellular $Ca^{2+}$ is involved in this cell death (Fig. 4); in yeast, $Ca^{2+}$ is stored in the vacuole at high concentrations.

It is likely that the vacuole is involved in the rapid cell death of *csg1*Δ *csh1*Δ cells under nitrogen starvation directly or indirectly, although we cannot exclude the involvement of other organelles. In this regard, then, we describe our working hypothesis for the molecular mechanism of the cell death as follows. Topologically, IPC is localized in the luminal (extracytosolic) leaflet of the lipid bilayers of the vacuolar membrane. Therefore, $Ca^{2+}$ may directly bind to IPC in the luminal leaflet, leading to destabilization of the vacuolar membrane. Indeed, we observed DCFDA and acidic contents flowing from the vacuole shortly before the collapse of intracellular structures in half of the nitrogen-deprived *csg1*Δ *csh1*Δ cells (Fig. 5B; pattern I). In these cells, the presence of cytoplasmic DCFDA signal was prolonged for a time after vacuole destruction, suggesting that the barrier function of the plasma membrane was still intact. Thus, in certain cells (pattern I) the vacuole seemed to be directly involved in cell death.

In contrast, in the rest of the cells (pattern II), disruption of vacuole membranes seemed to occur after cell death. In *csg1*Δ *csh1*Δ cells grown in the absence of nitrogen, cytoplasm became transparent and small, and the vacuoles were slightly swollen, and only later was the vacuole disrupted (Fig. 5B, lower panel). The initial morphological changes might represent plasma membrane collapse (Ohsumi *et al.* 1988), although other possibilities cannot be excluded. High concentrations of EGTA, which may represent endocytosed EGTA, and the removal of $Ca^{2+}$ from the medium prior to nitrogen starvation both suppressed cell death in *csg1*Δ *csh1*Δ cells under nitrogen-starved conditions (Fig. 4A and B). Thus, intracellular $Ca^{2+}$ apparently has important roles in nitrogen-deprived cell death, irrespective of the mechanisms of the cell death represented by the patterns in Fig. 5. The vacuole is the major $Ca^{2+}$ storage organelle and the final

destination for endocytosed materials. Therefore, it is likely that the vacuole is involved even in the cell death observed in pattern II, though probably through indirect effects; the precise mechanism, however, remains unclear. It is possible that decreased functioning of the vacuole or temporal disruption of the vacuole membrane causes changes in the cytosolic levels of $Ca^{2+}$, $H^{+}$, or other ions, which leads to the collapse of the plasma membrane or other organelles.

Although most IPC is localized in the plasma membrane under nutrient-rich conditions (Schneiter *et al.* 1999), we hypothesize that under nitrogen starvation IPC is transported to the vacuole, where it is available to bind to vacuolar $Ca^{2+}$. Proteins in the secretory pathway are redirected to the vacuole upon nitrogen starvation. For example, under these conditions, proteins localized in the ER and Golgi apparatus and secreted proteins are transported to the vacuole (van der Rest *et al.* 1995). In addition, the plasma membrane-localized amino acid permease Tat2 is delivered to the vacuole via endocytosis (Beck *et al.* 1999). To examine whether IPC localized in the plasma membrane is delivered to the vacuole upon nitrogen starvation via endocytosis, we examined the effects of mutations in endocytosis-related genes (*end3*Δ, *ede1*Δ, and *LAS17* tagged with a degron sequence) on the cell death of *csg1*Δ *csh1*Δ cells under nitrogen-starved conditions. However, introduction of either mutation had no effect (data not shown). Therefore, it is unlikely that IPC present in the plasma membrane is endocytosed under nitrogen-starved conditions. One cannot exclude the possibility, however, that residual endocytosis activity in those mutants was sufficient to induce the cell death. It is rather more likely, though, that under nitrogen-starved conditions newly synthesized IPC is delivered to the vacuole. Consistent with this notion, inhibition of *de novo* sphingolipid synthesis by myriocin suppressed the cell death (Fig. 3A).

We demonstrated here that *csg1*Δ *csh1*Δ *sur2*Δ cells are resistant to nitrogen starvation (Fig. 3B). Thus, phytosphingosine-containing IPC possesses higher cell death-inducible activity than does dihydrosphingosine-containing IPC. The difference between phytosphingosine and dihydrosphingosine is the presence of a hydroxyl group at the C4 position. One hydroxyl group can bind to another hydroxyl or amino group via a hydrogen bond. IPC species contain up to 4 additional such hydrogen bond-possible functional groups. Therefore, we speculate that IPC containing phytosphingosine has a high ability for

clustering in the membranes via hydrogen bonds. Since IPC also contains a phosphate group, it is most probable that the phosphate group binds to $Ca^{2+}$. In our working hypothesis, in the vacuole, $Ca^{2+}$ binding to IPC causes local disintegration of the putative IPC microdomain resulting in destruction of the vacuolar membrane. It is known that cells lacking MIPC synthase are sensitive to exogenous $Ca^{2+}$ (Beeler *et al.* 1994; Beeler *et al.* 1997; Uemura *et al.* 2003), although the precise underlying mechanism is unknown. Based on our model, we speculate that binding of $Ca^{2+}$ to the plasma membrane IPC microdomain causes plasma membrane destruction through a mechanism similar to our proposed destruction of the vacuolar membrane. In contrast to the MIPC synthase-deficient cells (*csg1*Δ *csh1*Δ), cells lacking $M(IP)_2C$ synthase (*ipt1*Δ) did not die under nitrogen-deprived conditions or in $Ca^{2+}$-high, nutrient-rich medium (data not shown). Since the difference between complex sphingolipids accumulating in these cells (IPC in the *csg1*Δ *csh1*Δ cells and MIPC in the *ipt1*Δ cells) is the presence of a mannose residue, it is possible that a mannose residue causes static hindrance and inhibits the putative binding of $Ca^{2+}$ to the phosphate group of MIPCs.

The rapid cell death of *csg1*Δ *csh1*Δ cells was observed under nitrogen-starved conditions, but not under nitrogen- and carbon-deprived conditions (Fig. 2B). Under nitrogen-starved conditions, energy is still produced from glucose. We revealed here that inhibition of energy production by $NaN_3$ suppressed the cell death under nitrogen starvation (Fig. 2D). Thus, energy-consuming processes such as transport of IPC to the vacuole or IPC synthesis may be required for the cell death.

In the presented study, we describe a phenomenon in which *csg1*Δ *csh1*Δ cells undergo rapid cell death upon nitrogen starvation. This cell death is caused by an accumulation of phytosphingosine-containing IPC. Thus, unperverted synthesis of complex sphingolipids is necessary for cell survival in nitrogen-depleted medium. This finding represents a novel function for sphingolipids, i.e., cell survival under nitrogen starvation conditions. Future studies expanding our knowledge of the detailed molecular mechanism behind the cell death described here will further our overall understanding of the roles of sphingolipids in responding to starvation conditions.

## Experimental procedures

### Yeast strains and media

*Saccharomyces cerevisiae* strains used in this study are listed in Table 1. All yeast cells used were derived from BY4741 (*MAT**a** his3Δ1 leu2Δ0 met15Δ0 ura3Δ0*) cells (Brachmann *et al.* 1998), obtained from Open Biosystems (Huntsville, AL). We used synthetic complete (SC) medium as a nutrient-rich medium, SC-$Ca^{2+}$ medium as a $Ca^{2+}$-absent, nutrient rich medium, synthetic dextrose (SD) medium without nitrogen (SD(-N)) as a nitrogen-deprived medium, synthetic medium without carbon (S(-C)) as a carbon-deprived medium, synthetic medium without nitrogen and carbon (S(-NC)) as a nitrogen- and carbon-deprived medium, and SD(-N)-$Ca^{2+}$ medium as a nitrogen- and $Ca^{2+}$-deprived medium. The composition of each medium is as follows: SC, 0.67% yeast nitrogen base without amino acids (Sigma, St. Louis, MO), 2% D-glucose, 0.5% casamino acid, 20 mg/l tryptophan, 20 mg/l adenine, and 20 mg/l uracil; SC-$Ca^{2+}$, 0.1% $KH_2PO_4$, 0.05% $MgSO_4$, 0.01% NaCl, 0.5% $(NH_4)_2SO_4$, 2 mg/l inositol, 2% D-glucose, 0.5% casamino acid, 20 mg/l tryptophan, 20 mg/l adenine, and 20 mg/l uracil; SD(-N), 2% D-glucose and 0.17% yeast nitrogen base without amino acids and ammonium sulfate (Wako, Osaka, Japan); S(-C), 0.5% ammonium sulfate and 0.17% yeast nitrogen base without amino acids and ammonium sulfate; S(-NC), 0.17% yeast nitrogen base without amino acids and ammonium sulfate; and SD(-N)-$Ca^{2+}$, 0.1% $KH_2PO_4$, 0.05% $MgSO_4$, 0.01% NaCl, 2 mg/l inositol, and 2% D-glucose. Cell culture was performed at 30 ˚C.

### Determination of cell survival rate

Cells grown to log-phase ($A_{600}$ >1) in SC medium were transferred to a nutrient-deprived medium and incubated for 4 or 24 hr. Cells were treated with 8 μg/ml phloxine B (Sigma; stock solution, 10 mg/ml in water) and subjected to microscopic observation under a DM5000B fluorescence microscope (Leica Microsystems, Wetzlar, Germany). Survival rates were calculated as living cells per total cells (at least 400 cells) after counting living and phloxine B-stained, dead cells.

### Imaging of the vacuole

Prior to staining with dichlorofluorescein diacetate (DCFDA), cells were grown to log-phase ($A_{600}$>1) in SC medium. Culture medium was then changed to SD(-N) medium containing 1 μM DCFDA (Wako; stock solution, 1 mM in DMSO). After a 3 hr incubation, cells were transferred to SD(-N) medium and photographed under a DM5000B fluorescence microscope. For staining with the lipophilic fluorescent dye FM4-64, cells grown to log-phase ($A_{600}$>1) in SC medium were treated for 30 min with 2 μM FM4-64 (Molecular Probes, Invitrogen, Eugene, OR; stock solution, 2 mM in ethanol). Cells were then washed with water, transferred to SD(-N) medium, incubated for 2.5 hr, and photographed under a DM5000B fluorescence microscope.

## Acknowledgements

We are grateful to Dr. E. A. Sweeney for scientific editing of the manuscript, to R. Obara for experimental support, and to Dr. S. Uemura (Aoyama Gakuin University) for discussion. This work was supported by a Grant-in-Aid for Scientific Research (B) (23370057) to AK and Grant-in-Aid for Young Scientists (B) (21770129) to KO from the Japan Society for the Promotion of Science (JSPS). This work was also supported by NISR Research Grants to KO from Noda Institute for Scientific Research.

## References


Aerts, A.M., Francois, I.E., Bammens, L., Cammue, B.P., Smets, B., Winderickx, J., Accardo, S., De Vos, D.E. & Thevissen, K. (2006) Level of $M(IP)_2C$ sphingolipid affects plant defensin sensitivity, oxidative stress resistance and chronological life-span in yeast. *FEBS Lett.* **580**, 1903-1907.

Alamgir, M., Erukova, V., Jessulat, M., Azizi, A. & Golshani, A. (2010) Chemical-genetic profile analysis of five inhibitory compounds in yeast. *BMC Chem. Biol.* **10**, 6.

Beck, T., Schmidt, A. & Hall, M.N. (1999) Starvation induces vacuolar targeting and degradation of the tryptophan permease in yeast. *J. Cell Biol.* **146**, 1227-1238.

Beeler, T., Gable, K., Zhao, C. & Dunn, T. (1994) A novel protein, CSG2p, is required for $Ca^{2+}$ regulation in *Saccharomyces cerevisiae*. *J. Biol. Chem.* **269**, 7279-7284.

Beeler, T.J., Fu, D., Rivera, J., Monaghan, E., Gable, K. & Dunn, T.M. (1997) *SUR1* (*CSG1*/*BCL21*), a gene necessary for growth of *Saccharomyces cerevisiae* in the presence of high $Ca^{2+}$ concentrations at 37 ˚C, is required for mannosylation of inositolphosphorylceramide. *Mol. Gen. Genet.* **255**, 570-579.

Brachmann, C.B., Davies, A., Cost, G.J., Caputo, E., Li, J., Hieter, P. & Boeke, J.D. (1998) Designer deletion strains derived from *Saccharomyces cerevisiae* S288C: a useful set of strains and plasmids for PCR-mediated gene disruption and other applications. *Yeast* **14**, 115-132.

Dickson, R.C., Nagiec, E.E., Wells, G.B., Nagiec, M.M. & Lester, R.L. (1997) Synthesis of mannose-(inositol-$P)_2$-ceramide, the major sphingolipid in *Saccharomyces cerevisiae*, requires the *IPT1* (*YDR072c*) gene. *J. Biol. Chem.* **272**, 29620-29625.

Dickson, R.C., Sumanasekera, C. & Lester, R.L. (2006) Functions and metabolism of sphingolipids in *Saccharomyces cerevisiae*. *Prog. Lipid Res.* **45**, 447-465.

Dunn, T.M., Haak, D., Monaghan, E. & Beeler, T.J. (1998) Synthesis of monohydroxylated inositolphosphorylceramide (IPC-C) in *Saccharomyces cerevisiae* requires Scs7p, a protein with both a cytochrome b5-like domain and a hydroxylase/desaturase domain. *Yeast* **14**, 311-321.

Haak, D., Gable, K., Beeler, T. & Dunn, T. (1997) Hydroxylation of *Saccharomyces cerevisiae* ceramides requires Sur2p and Scs7p. *J. Biol. Chem.* **272**, 29704-29710.

Hla, T. & Dannenberg, A.J. (2012) Sphingolipid signaling in metabolic disorders. *Cell Metab.* **16**, 420-434.

Im, Y.J., Idkowiak-Baldys, J., Thevissen, K., Cammue, B.P. & Takemoto, J.Y. (2003) *IPT1*-independent sphingolipid biosynthesis and yeast inhibition by syringomycin E and plant defensin DmAMP1. *FEMS Microbiol. Lett.* **223**, 199-203.

Kihara, A., Mitsutake, S., Mizutani, Y. & Igarashi, Y. (2007) Metabolism and biological functions of two phosphorylated sphingolipids, sphingosine 1-phosphate and ceramide 1-phosphate. *Prog. Lipid Res.* **46**, 126-144.

Klionsky, D.J., Cregg, J.M., Dunn, W.A., Jr., Emr, S.D., Sakai, Y., Sandoval, I.V., Sibirny, A., Subramani, S., Thumm, M., Veenhuis, M. & Ohsumi, Y. (2003) A unified nomenclature for yeast autophagy-related genes. *Dev. Cell* **5**, 539-545.

Mira, N.P., Lourenco, A.B., Fernandes, A.R., Becker, J.D. & Sa-Correia, I. (2009) The RIM101 pathway has a role in *Saccharomyces cerevisiae* adaptive response and resistance to propionic acid and other weak acids. *FEMS Yeast Res.* **9**, 202-216.

Mizutani, Y., Mitsutake, S., Tsuji, K., Kihara, A. & Igarashi, Y. (2009) Ceramide biosynthesis in keratinocyte and its role in skin function. *Biochimie* **91**, 784-790.

Nagiec, M.M., Nagiec, E.E., Baltisberger, J.A., Wells, G.B., Lester, R.L. & Dickson, R.C. (1997) Sphingolipid synthesis as a target for antifungal drugs. Complementation of the inositol phosphorylceramide synthase defect in a mutant strain of *Saccharomyces cerevisiae* by the *AUR1* gene. *J. Biol. Chem.* **272**, 9809-9817.

Ohsumi, Y. (1999) Molecular mechanism of autophagy in yeast, *Saccharomyces cerevisiae*. *Philos. Trans. R. Soc. Lond. B Biol. Sci.* **354**, 1577-1581.

Ohsumi, Y., Kitamoto, K. & Anraku, Y. (1988) Changes induced in the permeability barrier of the yeast plasma membrane by cupric ion. *J. Bacteriol.* **170**, 2676-2682.

Schneiter, R., Brugger, B., Sandhoff, R., Zellnig, G., Leber, A., Lampl, M., Athenstaedt, K., Hrastnik, C., Eder, S., Daum, G., Paltauf, F., Wieland, F.T. & Kohlwein, S.D. (1999) Electrospray ionization tandem mass spectrometry (ESI-MS/MS) analysis of the lipid molecular species composition of yeast

subcellular membranes reveals acyl chain-based sorting/remodeling of distinct molecular species en route to the plasma membrane. *J. Cell Biol.* **146**, 741-754.

Thumm, M., Egner, R., Koch, B., Schlumpberger, M., Straub, M., Veenhuis, M. & Wolf, D.H. (1994) Isolation of autophagocytosis mutants of *Saccharomyces cerevisiae*. *FEBS Lett.* **349**, 275-280.

Tsukada, M. & Ohsumi, Y. (1993) Isolation and characterization of autophagy-defective mutants of *Saccharomyces cerevisiae*. *FEBS Lett.* **333**, 169-174.

Uemura, S., Kihara, A., Inokuchi, J. & Igarashi, Y. (2003) Csg1p and newly identified Csh1p function in mannosylinositol phosphorylceramide synthesis by interacting with Csg2p. *J. Biol. Chem.* **278**, 45049-45055.

van der Rest, M.E., Kamminga, A.H., Nakano, A., Anraku, Y., Poolman, B. & Konings, W.N. (1995) The plasma membrane of *Saccharomyces cerevisiae*: structure, function, and biogenesis. *Microbiol. Rev.* **59**, 304-322.

van Meer, G. & Hoetzl, S. (2010) Sphingolipid topology and the dynamic organization and function of membrane proteins. *FEBS Lett.* **584**, 1800-1805.

Winzeler, E.A., Shoemaker, D.D., Astromoff, A. *et al.* (1999) Functional characterization of the *S. cerevisiae* genome by gene deletion and parallel analysis. *Science* **285**, 901-906.

Yamagata, M., Obara, K. & Kihara, A. (2011) Sphingolipid synthesis is involved in autophagy in *Saccharomyces cerevisiae*. *Biochem. Biophys. Res. Commun.* **410**, 786-791.

Zhao, C., Beeler, T. & Dunn, T. (1994) Suppressors of the $Ca^{2+}$-sensitive yeast mutant (*csg2*) identify genes involved in sphingolipid biosynthesis. Cloning and characterization of *SCS1*, a gene required for serine palmitoyltransferase activity. *J. Biol. Chem.* **269**, 21480-21488.

Zink, S., Mehlgarten, C., Kitamoto, H.K., Nagase, J., Jablonowski, D., Dickson, R.C., Stark, M.J. & Schaffrath, R. (2005) Mannosyl-diinositolphospho-ceramide, the major yeast plasma membrane sphingolipid, governs toxicity of *Kluyveromyces lactis* zymocin. *Eukaryot. Cell* **4**, 879-889.

## Figure legends

**Figure 1** Complex sphingolipids in yeast. The yeast *S. cerevisiae* contains three complex sphingolipids, IPC, MIPC, and $M(IP)_2C$. Synthesis of these lipid is catalyzed by Aur1, Csg1/Csg2 or Csh1/Csg2 complex, and Ipt1, respectively. Shown is the structure of $M(IP)_2C$. The 4-position of the long-chain moiety is hydroxylated by Sur2, whereas the α-position of the fatty acid portion is hydroxylated by Scs7. P, phosphate; Ino, inositol; Man, mannose.

**Figure 2** Rapid cell death of *csg1*Δ *csh1*Δ cells is induced upon nitrogen starvation. (A) BY4741 (WT) and MYY70 (*csg1*Δ *csh1*Δ) cells were grown to log-phase ($A_{600}$ >1) in SC medium then transferred to SD(-N) medium. After a 4 hr incubation, the cells were treated with 8 μg/ml phloxine B. Phase-contrast (PH) images and phloxine B staining were photographed using a DM5000B fluorescence microscope. Bar, 5 μm. (B) BY4741, MYY70, and 3267 (*atg14*Δ) cells grown to log-phase ($A_{600}$ >1) in SC medium were transferred to SC, SD(-N), S(-C), or S(-NC) medium. Four or twenty-four hr after incubation, the cells were treated with phloxine B and subjected to microscopic observation. Survival rates were calculated by counting living and phloxine B-stained, dead cells and are presented as a percentage of living cells per total cells. Values represent the mean ± S.D. from three independent experiments. (C) MYY70 cells were grown to log-phase ($A_{600}$ >1) in SC medium then transferred to SD(-N) medium containing the indicated concentration of glucose. After a 4 or 24 hr incubation, cell survival rates were determined as in (B). (D) MYY70 cells were grown to log-phase ($A_{600}$ >1) in SC medium then transferred to SD(-N) medium with or without 3 mM $NaN_3$. After a 4 hr incubation, the cells were stained with phloxine B and photographed as in (A). Merged images of phase-contrast and fluorescent images are presented. Bar, 5 μm. (E) MYY89 (*csg1*Δ *csh1*Δ) and MYY196 (*csg1*Δ *csh1*Δ *atg14*Δ) cells were grown to log-phase ($A_{600}$ >1) in SC medium. Cell medium was then changed to SD(-N) medium, and cells were incubated for 4 or 24 hr. Cell survival rates were determined as in (B). Values represent the mean ± S.D. from three independent experiments.

**Figure 3** Accumulation of phytosphingosine-containing IPC causes death of *csg1*Δ *csh1*Δ cells. (A)

BY4741 (WT) and MYY70 (*csg1*Δ *csh1*Δ) cells grown to log-phase ($A_{600}$>1) in SC medium were treated with 5 μM myriocin or methanol (mock treatment) for 30 min. Cells were then transferred to SD(-N) medium with or without 5 μM myriocin and incubated for 4 or 24 hr. Cells were treated with 8 μg/ml phloxine B, observed under a microscope. Survival rates were calculated by counting living and phloxine B-stained, dead cells and are presented as a percentage of living cells per total cells. Values represent the mean ± S.D. from three independent experiments. Statistically significant differences are indicated (*p<0.05; t-test). Myr, myriocin. (B) MYY89 (*csg1*Δ *csh1*Δ), MYY102 (*csg1*Δ *csh1*Δ *sur2*Δ), MYY321 (*csg1*Δ *csh1*Δ *scs7*Δ), and MYY104 (*csg1*Δ *csh1*Δ *ccc2*Δ) cells were grown to log-phase ($A_{600}$>1) in SC medium. Cells were then incubated in SD(-N) medium for 4 or 24 hr, and were subjected to phloxine B treatment and microscopic observation. Cell survival rates were determined as in (A). Statistically significant differences are indicated (*p<0.05, **p<0.01; t-test).

**Figure 4** Intracellular $Ca^{2+}$ is involved in the death of *csg1*Δ *csh1*Δ cells under nitrogen starvation conditions. (A) BY4741 (WT) and MYY70 (*csg1*Δ *csh1*Δ) cells grown to log-phase ($A_{600}$>1) in SC medium were transferred to SD(-N) medium containing the indicated concentration of EGTA. Four or twenty-four hr after incubation, cells were treated with 8 μg/ml phloxine B, observed under a microscope. Survival rates were calculated by counting living and phloxine B-stained, dead cells and are presented as a percentage of living cells per total cells. Values represent the mean ± S.D. from three independent experiments. Statistically significant differences are indicated (*p<0.05, **p<0.01; t-test). (B) BY4741 and MYY70 cells were grown for 5 hr to early log-phase ($A_{600}$>1) in SC medium with or without $Ca^{2+}$ as indicated. Cells were then incubated with SC, SD(-N), SD(-N)-$Ca^{2+}$, or SC-$Ca^{2+}$ medium as indicated for 4 or 24 hr. Cell survival rates were calculated after phloxine B staining and microscopic observation and are presented as in (A). -N, SD(-N).

**Figure 5** The vacuole is collapsed prior to death in half of *csg1*Δ *csh1*Δ cells cultured under nitrogen-deprived conditions. (A) BY4741 (WT) and MYY70 (*csg1*Δ *csh1*Δ) cells grown to log-phase

($A_{600}$>1) in SC medium were stained with 2 μM FM4-64 for 30 min, washed with water, transferred to SC or SD(-N) medium, incubated for 2.5 hr, and photographed under a DM5000B fluorescence microscope. Bar, 5 μm. (B) MYY70 cells were grown to log-phase ($A_{600}$>1) in SC medium. Culture medium was then changed to SD(-N) medium containing 1 μM DCFDA which yields fluorescence under acidic conditions. After a 3 hr incubation, cells were transferred to fresh SD(-N) medium without DCFDA and photographed at 2 min intervals under a DM5000B fluorescence microscope. Examples of two patterns indicative of different modes of death (patterns I and II) are presented. The time at which the first morphological change was observed was set as 0 min. The number above each cell image represents the minutes after the first morphological change. -N, SD(-N); PH, phase-contrast.

Fig. 1

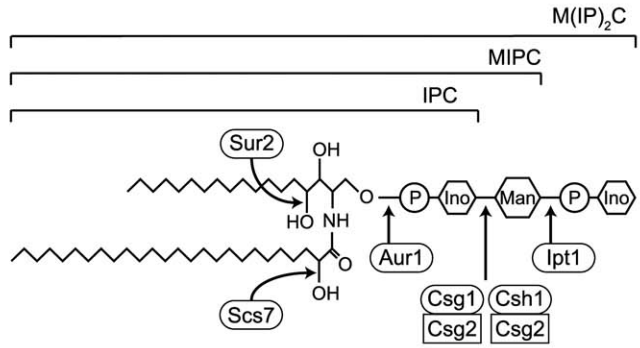
M(IP)2C
MIPC
IPC
Sur2
OH
HO
NH
O
P
Ino
Man
P
Ino
Aur1
Ipt1
Csg1
Csh1
Csg2
Csg2
O
OH
Scs7

Fig. 2

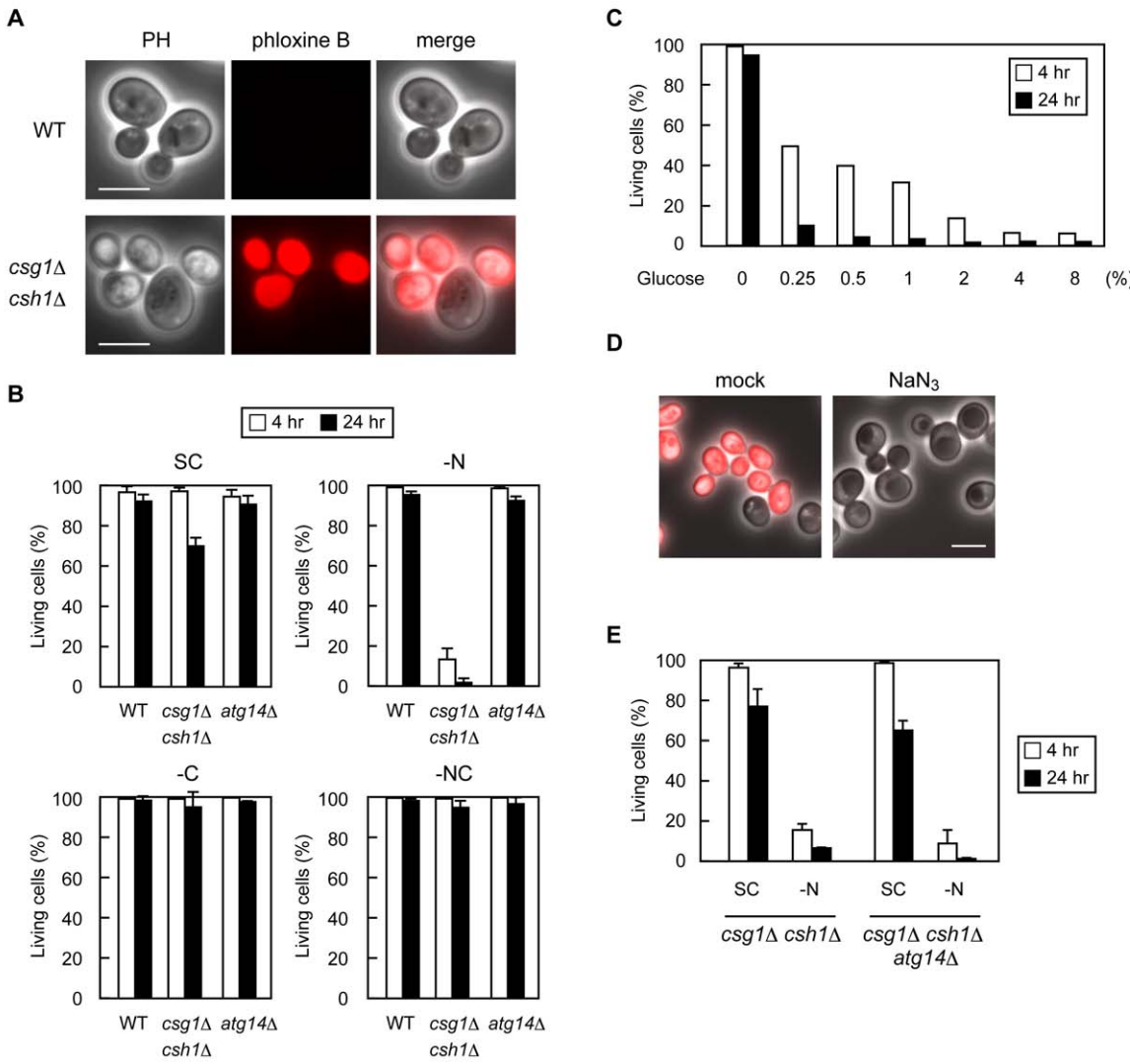
A
PH
phloxine B
merge
WT
csg1Δ csh1Δ
B
4 hr
24 hr
SC
-N
-C
-NC
Living cells (%)
WT
csg1Δ csh1Δ
atg14Δ
C
Living cells (%)
Glucose
0
0.25
0.5
1
2
4
8
(%)
D
mock
NaN3
E
Living cells (%)
SC
-N
csg1Δ csh1Δ
csg1Δ csh1Δ atg14Δ

Fig. 3

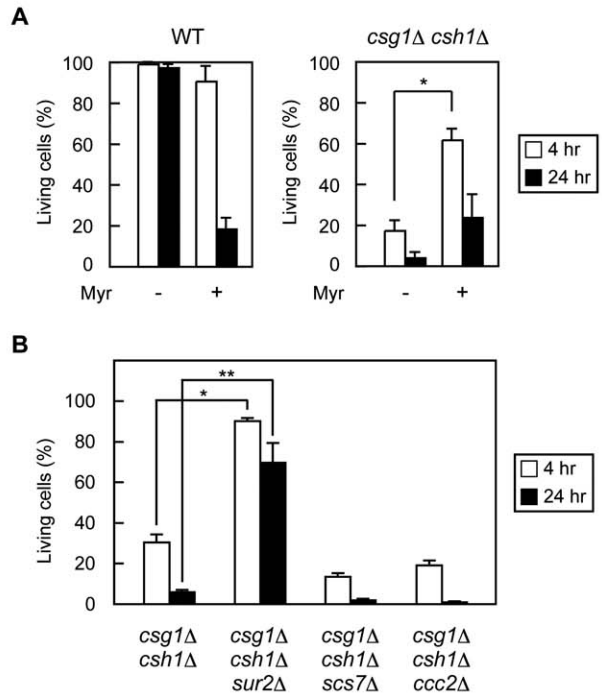
A
WT
csg1Δ csh1Δ
Living cells (%)
100
80
60
40
20
0
Myr
-
+
*
4 hr
24 hr
B
**
*
csg1Δ csh1Δ
csg1Δ csh1Δ sur2Δ
csg1Δ csh1Δ scs7Δ
csg1Δ csh1Δ ccc2Δ

Fig. 4

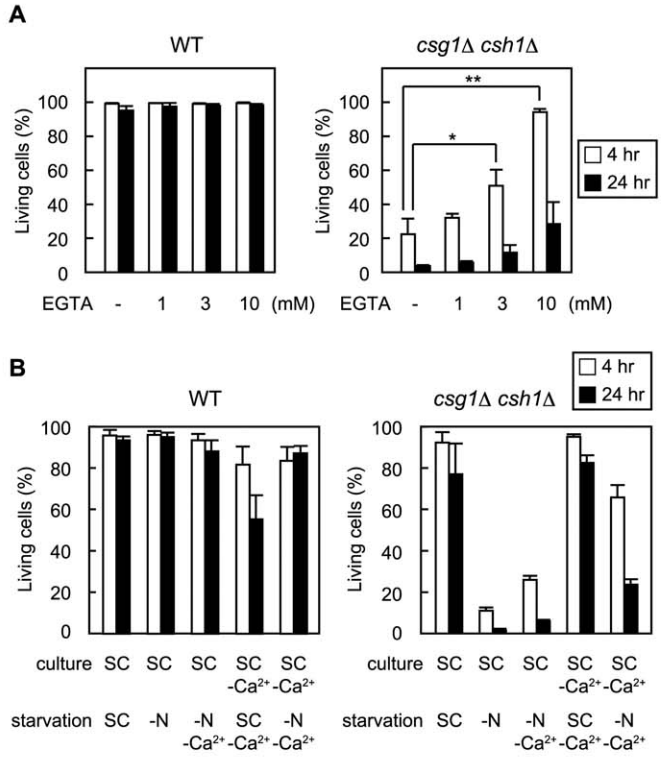
A
WT
csg1Δ csh1Δ
Living cells (%)
100
80
60
40
20
0
**
*
4 hr
24 hr
EGTA - 1 3 10 (mM)
B
culture SC SC SC SC SC
-Ca2+ -Ca2+
starvation SC -N -N SC -N
-Ca2+ -Ca2+ -Ca2+

Fig. 5

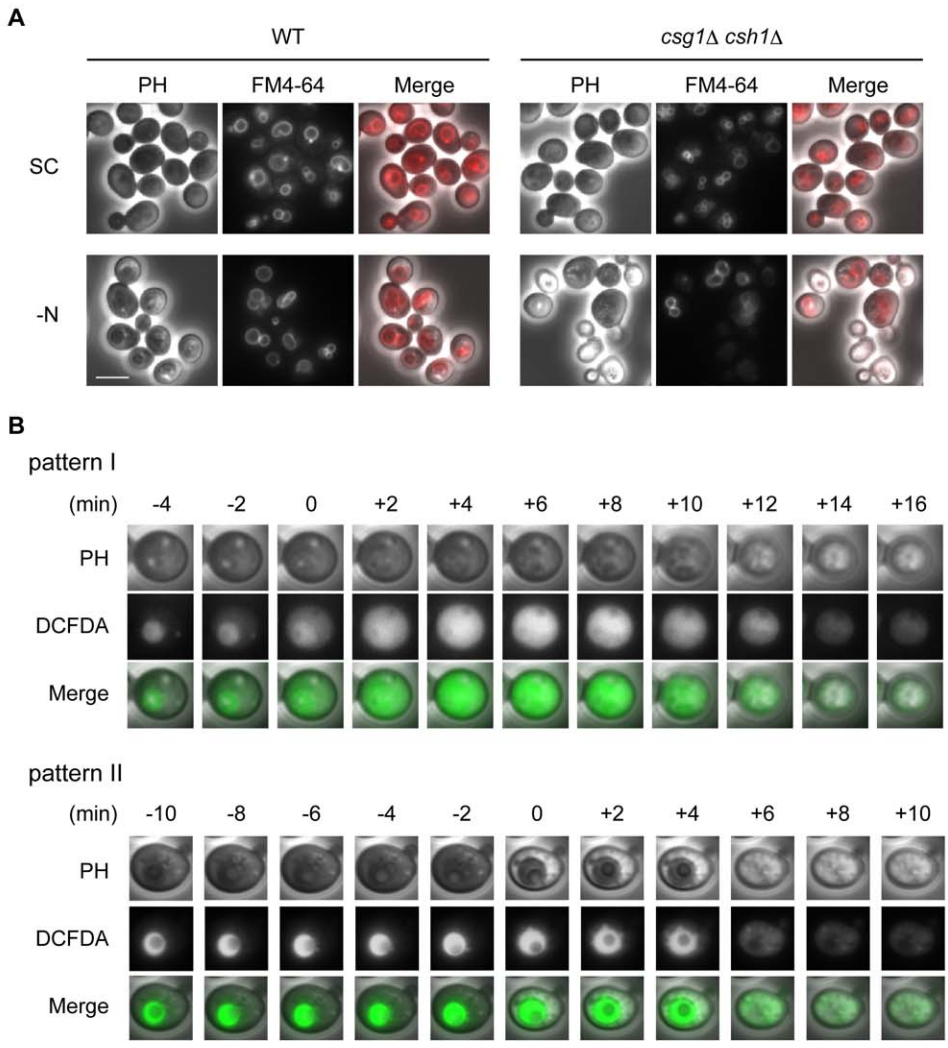
A
WT
csg1Δ csh1Δ
PH
FM4-64
Merge
PH
FM4-64
Merge
SC
-N
B
pattern I
(min) -4 -2 0 +2 +4 +6 +8 +10 +12 +14 +16
PH
DCFDA
Merge
pattern II
(min) -10 -8 -6 -4 -2 0 +2 +4 +6 +8 +10
PH
DCFDA
Merge